Persicaria minor F-box Gene *PmF-box1* Indirectly Affects *Arabidopsis thaliana* LOX-HPL Pathway for Green Leaf Volatile Production

(*Persicaria minor* F-box Gene *PmF-box1* Secara Tidak Langsung Mempengaruhi *Arabidopsis thaliana* Laluan LOX-HPL untuk Pengeluaran Daun Hijau Meruap)

Nur-Athirah Abd-Hamid[1], Muhammad Naeem-Ul-Hassan[2,3], Zamri Zainal[1,2] & Ismanizan Ismail[1,2,*]

[1]*Institute of Systems Biology (INBIOSIS), Universiti Kebangsaan Malaysia, 43600 UKM Bangi, Selangor, Malaysia*
[2]*Department of Biological Sciences and Biotechnology, Faculty of Science and Technology, Universiti Kebangsaan Malaysia, 43600 UKM Bangi, Selangor, Malaysia*
[3]*Department of Chemistry, University of Sargodha, Sargodha, Punjab 40100, Pakistan*

ABSTRACT

Green leaf volatiles (GLVs) play an essential role in plant defence, plant-plant interaction and plant-insect interaction. The plant releases GLVs and inhibits the growth and propagation of plant pathogens. In this study, overexpression of *PmF-box1* in wild type *A. thaliana* showed the downregulation of genes involved in the lipoxygenase-hydroperoxide lyase (LOX-HPL) pathway, which contributes to the biosynthesis of GLVs. It resulted in a marked reduction of hexanal production in the *PmF-box1*-overexpressing plant. The expression pattern of LOX-HPL branch genes in the kelch-repeat modified *PmF-box1 (KMF)*-overexpressing plant showed a pattern much closer to the expression of LOX-HPL branch genes in the vector control (VC) plant. It was shown that the functional KMF protein sequence was not responsible for the significant reduction of all GLVs including hexanal, 1-hexanol, (Z)-3-hexen-1-ol, and the carbon 5 (C5) volatile, 1-penten-3-ol, in plants overexpressing *KMF*. Furthermore, this study also showed that the relative proportion of production of 1-penten-3-ol to hexanal was higher in the *PmF-box1*-overexpressing plant. Based on the current comparative literature search, *PmF-box1* does not appear to interact directly with the proteins or transcription factors of the LOX-HPL pathway. On the other hand, *PmF-box1* interacts with SAMS1, which subsequently influences the HPL pathway enzyme genes. Thus, this study highlights the potential roles of *PmF-box1* in the manipulation of GLV productions.

Keywords: F-box proteins; hydroperoxide lyase; Kelch-repeats; lipoxygenase; oxylipin

ABSTRAK

Sebatian meruap daun hijau (GLV) memainkan peranan penting dalam pertahanan tumbuhan, interaksi tumbuhan-tumbuhan dan interaksi tumbuhan-serangga. Tumbuhan membebaskan GLV serta merencat pertumbuhan dan propagasi patogen tumbuhan. Dalam kajian ini, pengekspresan lampau *PmF-box1* dalam *A. thaliana* jenis liar telah menunjukkan pengawalaturan menurun gen yang terlibat dalam tapak jalan lipoksigenase-hidroperoksid liase (LOX-HPL) yang menyumbang kepada biosintesis GLV. Ia mengakibatkan pengurangan penghasilan heksanal yang ketara dalam tumbuhan yang mengekspres *PmF-box1* secara melampau. Corak pengekspresan gen cabang LOX-HPL dalam tumbuhan yang mengekspres *PmF-box1* secara melampau dengan ulangan Kelch (*KMF*) yang terubah suai menunjukkan corak pengekspresan yang hampir sama dengan gen cabang LOX-HPL di dalam tumbuhan kawalan vektor (VC). Ini menunjukkan bahawa jujukan protein KMF yang berfungsi tidak bertanggungjawab terhadap penurunan yang signifikan bagi semua GLV termasuk heksanal, 1-heksanol, (Z)-3-heksen-1-ol dan karbon 5 (C5) meruap, 1-penten-3-ol, di dalam tumbuhan yang mengekspreskan *KMF* secara melampau. Tambahan pula, kajian ini juga menunjukkan bahawa perkadaran relatif penghasilan 1-penten-3-ol kepada heksanal adalah lebih tinggi di dalam tumbuhan yang mengekspres *PmF-box1* secara melampau. Berdasarkan carian perbandingan kepustakaan semasa, *PmF-box1* didapati tidak dapat berinteraksi secara langsung dengan protein atau faktor transkripsi bagi tapak jalan LOX-HPL. Sebaliknya, *PmF-box1* berinteraksi dengan SAMS1, yang kemudiannya mempengaruhi gen enzim tapak jalan HPL. Oleh itu, kajian ini menunjukkan *PmF-box1* berpotensi berperanan dalam memanipulasi penghasilan GLV.

Kata kunci: Hidroperoksid liase; lipoksigenase; oksilipin; protein F-box; ulangan Kelch

Introduction

Persicaria minor (Huds.), also known as *Polygonum minus*, belongs to the Polygonaceae family, and the plant is native to Southeast Asian countries such as Indonesia, Thailand, Vietnam and Malaysia. In Malaysia, the plant is known as 'Kesum' or 'Laksa leaves' and due to its pleasant and sweet aroma, it is a common ingredient in some Malaysian delicacies, like salad and laksa. It has been used for centuries as a folk remedy to treat digestive disorders, dandruff, and improve vision. The plant has been found to contain a high level of flavonoids and essential oil rich in volatile compounds (Vikram et al. 2014). Using spectroscopic techniques, Christapher et al. (2015) have identified about 69 compounds from the essential oil of *P. minor* that impart most of the aroma of the plant (Christapher et al. 2015). These volatile compounds mainly comprises flavonoids and green leaf volatiles (GLVs), which are emitted immediately in response to biotic and abiotic stresses (Naeem-Ul-Hassan et al. 2015). GLVs are phyto-oxylipins that protect the plants against herbivory and other pathogen invasions and serve as aerial messengers for communication among plant communities (Engelberth et al. 2013, 2004; Gershenzon 2007). GLV formation is mediated through the oxylipin pathway of the LOX-HPL branch. The subclass of GLVs includes some carbon 6 (C6) and carbon 9 (C9) aldehydes and alcohols, and their derivatives with fresh green fragrances (Vincenti et al. 2019). In addition, C5 volatiles, known as pentyl leaf volatiles (PLVs), are also commonly emitted through LOX-HPL-derived volatile oxylipins (Gorman et al. 2021). However, Sarang et al. (2021) collectively referred to C6 and C5 volatile compounds as GLVs.

The ubiquitin-26S proteasome system (UPS), through recognition by a specific F-box protein (FBP), is one of the most common protein degradation signalling pathways. FBP acts in protein-protein interaction, a well-known function in the SCF complex. SCF is a multi-subunit E3 ubiquitin ligase that comprises four main components namely Skp1, Cullin, F-box and Rbx1, which also contribute to the complex name. Since the discovery of the F-box protein (Bai et al. 1996), researchers all around the world have identified a large number of FBPs, particularly in plants. However, the majority of these FBPs are either 'orphans' or their function has not been fully elucidated until today.

FBPs containing kelch-repeats (FBK or KFB) receive high interest from plant biologists and biochemists due to the fact that they are one of the most common FBPs in planta. FBK is an overrepresented subfamily in plants relative to other kingdoms. No FBK genes have been identified in prokaryotes, whereas the majority of non-plant eukaryotes possess a single FBK gene. The high presence of FBKs in plants indicates that FBKs play a significant role in various processes in plants. Abd-Hamid et al. (2020) listed 15 FBKs involved in various plant functions which are secondary metabolite production, stress responses, phytohormone biosynthesis, senescence, pollen recognition, seed germination, plant development, miRNA biogenesis, light signalling and photoperiodism. The involvement of FBKs in various plant functions shows the importance of this subfamily for the plant to grow normally.

Previous studies in our laboratory had discovered and structurally characterised a novel F-box gene in *P. minor* called *PmF-box1*. Upregulation of the *PmF-box1* gene was observed in the *P. minor* plants due to the exogenous application of jasmonic acid (Gor et al. 2010). Analysis of the *PmF-box1* gene sequence with GenBank identification number JQ429325 has revealed that it encodes 487 amino acids of an FBK protein with two kelch-repeats (Othman et al. 2017). Additionally, in the same research, *PmADH1* and *PmLOX1* were elevated by jasmonic acid. In Arabidopsis, SKP1 interacting protein 11 (SKIP11) (AT2G08270) is one of the homologs with the highest sequence similarity and identity to PmF-box1 through Blast search analysis. *A. thaliana* SKIP11 is a 467-amino acid containing F-box protein with five kelch-repeat motifs. Recently, we documented the function of the *AtSKIP11* gene in the oxylipin pathway for GLV production (Naeem-Ul-Hassan et al. 2017). These observations led us to recommend that *PmF-box1* may also be involved in the *P. minor* oxylipin pathway, specifically in the production of GLVs. The present study aimed to investigate the functions of *PmF-box1* in the HPL branch (LOX2-HPL) of the oxylipin pathway.

Materials and Methods

PmF-box1 SEQUENCE ANALYSIS AND PHYLOGENETIC TREE CONSTRUCTION

Blastx analysis was conducted on the NCBI database to gain more information on the *PmF-box1* gene. Several plants from dicot and monocot plants, including Arabidopsis and Rice were chosen, and only sequences with 99% query coverage were selected for phylogenetic analysis. Phylogenetic analysis was conducted using MEGA 11, where multiple sequence alignment was first created in MEGA 11 using the MUSCLE algorithm. Next, a phylogenetic tree was constructed using the Neighbor-

Joining method with 1000 bootstrap replications, and the Poisson correction method was used to compute the evolutionary distances.

CONSTRUCTION OF *PmF-box1* OVEREXPRESSION VECTOR

The *PmF-box1* nucleotide sequence was obtained from the NCBI database using the identification number JQ429325. The preparation of a high-quality cDNAtemplate was accomplished through the purification of total RNA from *P. minor* plant samples, followed by the elimination of gDNA contamination and cDNA synthesis, following the protocols reported by Naeem-Ul-Hassan et al. (2017). This cDNA was used as a template to amplify a 1,530 bp full-length ORF of the *PmF-box1* gene using PCR with a set of primers containing gateway attB sites (Table 1).

The PCR reaction was conducted on an Eppendorf master cycler machine with Platinum Taq DNA polymerase (Life Technologies, US) using the PCR program that consisted of one cycle of initial denaturation at 94 °C for 2 min, 30 cycles of denaturation at 94 °C for 15 s, primer annealing at 55 °C for 30 s and strand elongation at 68 °C for 1.5 min. The PCR product was then purified using a Purelink PCR purification kit (Invitrogen, US) according to the manufacturer's instructions. Next, using the Gateway cloning system (Invitrogen, US), pENTR_*PmF-box1* was produced before the *PmF-box1* was further cloned into the destination vector, pB2GW7, to produce the overexpression vector pB2GW7_*PmF-box1*.

CONSTRUCTION OF KELCH-REPEAT MODIFIED *PmF-box1* (*KMF)* OVEREXPRESSION VECTOR

The 24 bp sequence (eight amino acid residues) deletion in the first kelch-repeat to generate the first kelch-repeat modified *PmF-box1* (K_1MF) sequence, the entry clone pENTR_*PmF-box1*, which was prepared in the previous section was used. The sequence deletion was generated using the Q5® site-directed mutagenesis kit (NEB, USA), according to the manufacturer's protocol. Briefly, the forward and reverse primers, shown in Table 2, were designed by the NEBase changer tool to amplify using PCR the whole sequence except the area to be deleted from the ORF.

In a PCR tube, a 25 µL reaction was prepared using Q5® Hot Start High-Fidelity 2X Master Mix. The following PCR program was conducted for the amplification of the desired sequenc which consisted of one cycle of initial denaturation at 98°C for 30 seconds, 25 cycles of denaturation at 98 °C for 10 s, annealing at 63 °C for 30 s, extension at 72 °C for 2.5 min and one cycle of final extension at 72 °C for 3 min. The PCR product was then subjected to the Kinase, Ligase & DpnI (KLD) reaction treatment as stated in the mutagenesis kit protocol mentioned above.

TABLE 1. Primer sequences utilised in the synthesis of cDNA inserts for the construction of pB2GW7_*PmF-box1*

Primer	Sequence (5' – 3')	Amplicon size
PmF-box1-attB1(F)	GGGGACAAGTTTGTACAAAAAAGCAGGCTTCGAAGGAGATAGAATGTTGGAGGATCACTCTTGTCTGG	
PmF-box1-attB2(R)	GGGGACCACTTTGTACAAGAAAGCTGGGTCTTAACACCCCATCACCGCACAGT	1530 bp

TABLE 2. Primers for the site-directed mutagenesis-mediated deletion of specified sequence from the first and second kelch-repeats of *PmF-box1*

Deletion of	Primer name	Sequence (5' – 3')
1st kelch-repeat	KMF-sdmF1	GAAGTTCTTCCTGACATGATTAAACC
	KMF-sdmR1	GAGCTCAGCAGAACTGCG
2nd kelch-repeat	KMF-sdmF2	AAGGAAATTCCAAACATGTC
	KMF-sdmR2	CTCCTCAGCACTAGTCAAG

About 5 µL of the KLD reaction mixture was transformed into Top10 *E. coli* competent cells, and the culture was grown overnight at 37 °C on LB agar plates containing kanamycin. Colony PCR screening was performed to confirm the presence of the pENTR_K_1MF recombinant plasmid. After confirmation of the construct, positive colonies were further grown, and the plasmid was isolated using the PureLink Plasmid Miniprep Kit (Invitrogen, USA) and further verified by sequencing.

After the first kelch-repeat deletion was produced, another deletion of the 24-bp sequence (eight amino acid residues) on the second kelch-repeat was generated by mutagenising the pENTR_K_1MF to generate *KMF*. The *KMF* is now a sequence with modified kelch at the first and second kelch-repeats of the *PmF-box1* sequence. Using the Q5 site-directed mutagenesis kit from NEB, the required sequence was deleted from the second kelch-repeat, as described earlier. The forward and reverse primers shown in Table 2 were designed by the NEBase changer tool to amplify the whole sequence except the area to be deleted from the ORF by using PCR. The PCR program and the PCR product's KLD treatment were performed following the same protocol as given above.

After the pENTR_*KMF* recombinant plasmid was produced, an LR clonase reaction from the Gateway cloning system was carried out to transfer the *KMF* fragment from the entry clone, pENTR_*KMF*, to the destination vector, pB2GW7. The resulting recombinant plasmid, pB2GW7_*KMF,* was used for transformation into Top 10 *E. coli* competent cells and the subsequent antibiotic selection of the successful transformants was conducted. Confirmation of the integration of the *KMF* sequence in the recombinant plasmid was accomplished through colony PCR and sequencing analysis. The deletion sites on the *PmF-box1* sequence can be reviewed in supplementary material (Figure S1).

GENERATION OF TRANSGENIC *A. thaliana* PLANTS OVEREXPRESSING *PmF-box1* GENE AND *KMF*

Both overexpression constructs, pB2GW7_*PmF-box1* and pB2GW7_*KMF* were transformed into *Agrobacterium tumefaciens* strain GV3101 separately, prior to the floral dip transformation of *A. thaliana* (Clough & Bent 1998). Putative transformants were cultivated in the growth chamber (conviron), and the selection was made using the herbicide 'glufosinate' (Basta) because the recombinant plasmid contains a bar gene. PCR analysis using the genomic DNA as the template and the primers provided in Table 3 validated the transgene incorporation in the putatively transgenic *A. thaliana* plants that survived the repeated herbicide sprays on alternate days.

GENE EXPRESSION AND METABOLIC ANALYSIS OF THE TRANSGENIC *A. thaliana* PLANTS INTEGRATING *PmF-box1* GENE AND *KMF*

On soil, transgenic *A. thaliana* plants were cultivated to maturity until T_2 seeds were harvested. Gene expression and metabolic studies were conducted on transgenic plants of the T_2 generation. Using the T_3 generation of transgenic plants is unarguably the best option for analysing any metabolic pathway because the representative plants are homozygous. However, analysis of T_2 generation for studying the pathways at genetic and metabolic levels is also prevalent (Feng et al. 2014; Wang et al. 2011; Zhang et al. 2013). Following the classical Mendelian pattern, T_2 generation will produce transformed plants in a ratio of 1:2:1 (homozygous recessive (non-transformant): heterozygous: homozygous dominant). During the screening of transgenic plants by PCR using the plant gDNA as a template, only plants with a very clear, dense band were selected for functional analysis. Two of the

TABLE 3. Primers for transgene validation in putative transgenic Arabidopsis

Primer	Sequence (5' – 3')	Amplicon size
PmF-box1-F2 (pB2GW7 specific)	CCGTGAAGACTGGCGAACA	
		≈760
PmF-box1-R2 (*PmF-box1*/ KMF specific)	CCGCTCTCTTCCTCTTCTGCT	

transgenic events from each of the *PmF-box1* overexpressing and the kelch-modified *PmF-box1* (*KMF*) plants were chosen for further examination by real-time quantitative PCR (RT-qPCR) and solid phase micro-extraction gas chromatography mass spectrophotometer (SPME-GCMS) following methods in Naeem-Ul-Hassan et al. (2017). Control plants overexpressing the empty vector pB2GW7 (VC) were also cultivated alongside the transgenic plants. For gene expression analysis, the LOX-HPL branch genes of the oxylipin pathway, which are *AtLOX2* (At3g45140) and *AtHPL* (At4g15440) were analysed, and *Actin 2* (At3g18780) was used as the reference gene. The primer sequences used were the same as in Naeem-Ul-Hassan et al. (2017).

RESULTS AND DISCUSSION

ANALYSIS OF *PmF-box1* HOMOLOGS FROM OTHER PLANTS TO PREDICT ITS RELATED FUNCTION

For the construction of the phylogenetic tree, 20 *PmF-box1* homolog sequences were selected from the Blastx

results. As seen in the phylogenetic tree in Figure 1, the protein sequences of monocot and dicot plants were separated into two groups. For the dicots, two subgroups were formed. The *PmF-box1* is included in Subgroup I, which is in the same group as *Arabidopsis thaliana*. *PmF-box1* has 68% sequence similarity and 56% sequence identity, with both At1g14330 and At2g02870. Nevertheless, the E-value for At1g14330 is the lowest, 5e-174, whereas the E-value for At2g02870 is 2e-172. As shown in Figure 1, At1g14330 and At2g02870 form a paralog gene pair in Arabidopsis. Compared to the F-box protein of *Oryza sativa* (rice), which is OsFBK12 with *PmF-box1*, the sequence similarity is 64%, and sequence identity is 52% with an E-value of 2e-158.

Furthermore, when a comparison was made between OsFBK12 and At1g14330, it produced 68% similarities and 54% identities with the E-value 5e-166. In contrast, the comparison of OsFBK12 to At2g02870 produced similarities of 66% and identities of 53% with the E-value 1e-159. At2g02870 has sequence similarity and identity of 81% and 74%, respectively, with At1g14330. To date, only At2g02870, also known
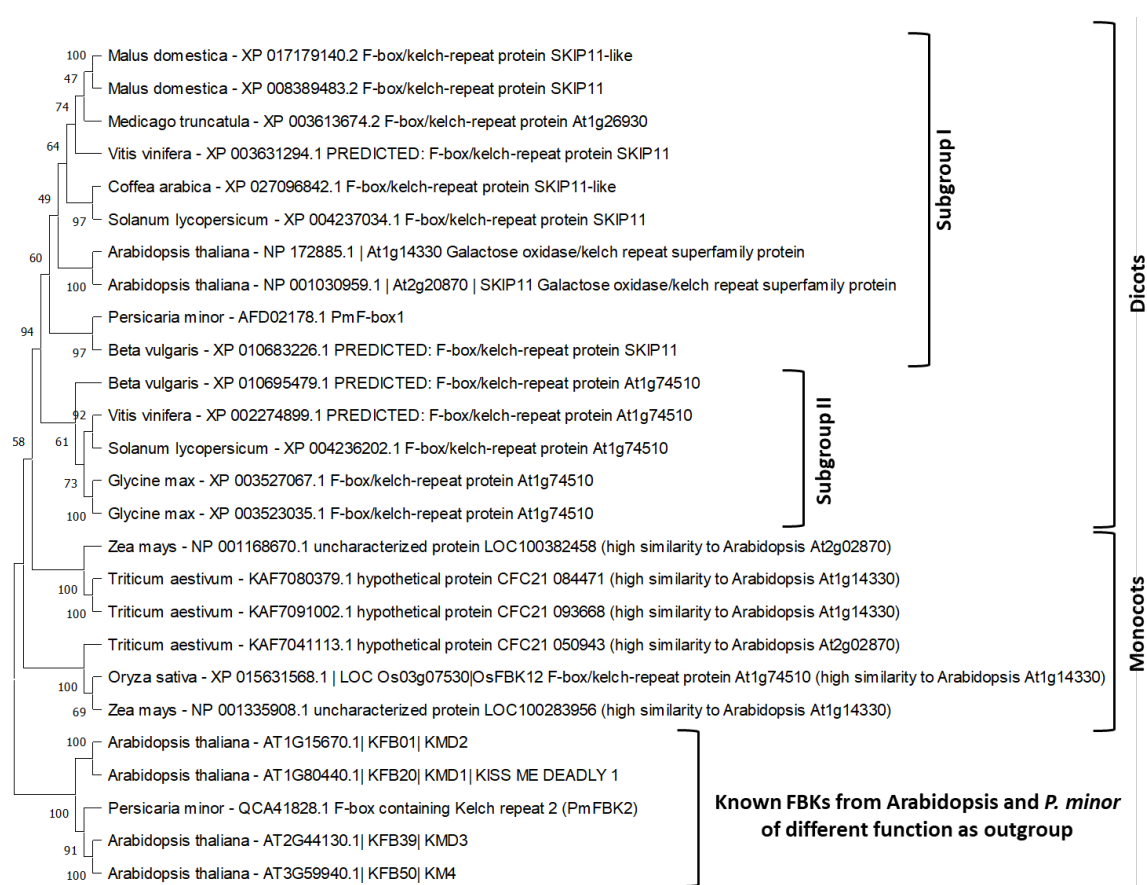

FIGURE 1. Phylogenetic analysis of PmF-box1 protein homologs from different plants

as SKP1-interacting partner 11 (SKIP11)/ AtARKP1 has been subjected to further analysis (Li et al. 2015; Risseeuw et al. 2003). With the high sequence identities and similarities between At2g02870 and At1g14330, these two genes might form a multigene family with similar functions in the Arabidopsis.

Figure 2 depicts a multiple sequence alignment using MUSCLE of the four F-box protein sequences, PmF-box 1, At1g14330, At2g02870 and OsFBK12.

The percentage of similarity between the sequences is relatively high. The high sequence similarity allows us to predict the function of PmF-box1 through comparison with its homolog. F-box protein is best known as a component of the SCF complex, which is involved in protein-protein interaction, and post-translational regulation. The SCF complex is a multisubunit E3 ubiquitin ligase. With the aid of F-box protein, it will recognise and target the protein to be ubiquitinated,

```
CLUSTAL multiple sequence alignment by MUSCLE (3.8)


OsFBK12             MMLEGN---SCLISRSLPSSCEPESQW----------AYLSHEVLNGKRPAPEDAEA---
PmF-box1            -MLEDH---SCLVSRALQSSCEQESKW------PYAKCGLEAVVSKGKRPLDSEAEEEES
At1g14330           -MVEDR---TYLMSRIFSSSRLSESKW--PYMYPQPEDSSESNLINGKRALENDVDE---
At2g20870|SKIP11    -MLEDRSPDSCLSTRVFSSSRLSESNWSNSYMYPEDDDKL---LGNGKRALEVVGEV---
                     *:*..   : * :* : **   **:*          : :***.    :


OsFBK12             ---------------EDMDEVDF------GGGKRSKPPSPQPH---------------TP
PmF-box1            GSRKSAKLSDIMGEVQSINIQSYSSL--EGGGERINSGDQHQAGNPPSAQFVDQQQGGDP
At1g14330           -----------LRQSKSPRLMGFSI----HGNEAIEEDEQEQ------------------
At2g20870|SKIP11    ------------RQTKSLKLMGFSIIYDSDSSDYSLSGGEEQA---------------DA
                                   :.     .:     ...


OsFBK12             DISEG----HGSSRHVAASGGGEEHGNGSSLIGAIGRDLTINCLLRLSRSDYGSVASLNK
PmF-box1            PSAQTGEQQQGGDDQPGDQQQGGDQSDTDNLIHPIGRDITINCLLHCSRADYGSIASLNR
At1g14330           -------------DQSDSNNNG--NSDGDSLINDIGRDNSISCLIRCSRSGYGSIASLNR
At2g20870|SKIP11    AIGDGSSSRQEQEQQSDFNDNGGDSSDSHSLINEIGRDNSIDCLIRCSRSDYGSIASLNR
                                 :   .  *   .:   .**  ****  :*.**:. **:.***:****.


OsFBK12             DFRSLVRNGEIYRLRRQSGVAEHWVYFSCNVLEWDAYDPYRERWIQVPKMPPDECFMCSD
PmF-box1            GFRSLVRSGEMYKLRRMNGVVEHWVYFSCQLLEWVAFDPVARRWMNLPRMNVNECFMCSD
At1g14330           SFRSLVKTGEIYRLRRQNQIVEHWVYFSCQLLEWVAFNPFERRWMNLPTMPSGVTFMCAD
At2g20870|SKIP11    NFRSLVKSGEIYRLRRQNGFVEHWVYFSCQLLEWVAFDPVERRWMQLPTMPSSVTFMCAD
                    .***** .**:*.***  . .********:.*** *::*    **::* *  .  ***:*


OsFBK12             KESLAVGTELLVFAM----AHIVFRYSILTNSWTRADPMISPRCLFGSTSVGAKAYVAGG
PmF-box1            KESLAVGTQLLLFGK-EVTSHVMYKYSILTNSWSLGDMMNAPRCLFGSASLGHIAILAGG
At1g14330           KESLAVGTDLLVLGKDDYSSHVIYRYSLLTNSWSSGMRMNSPRCLFGSASLGEIAIFAGG
At2g20870|SKIP11    KESLAVGTDLLVLGKDDFSSHVIYRYSLLTNSWSSGMKMNSPRCLFGSASLGEIAIFAGG
                    ********:**::.     :*:::.**.*****: .  * :*******.*:*  *  .***


OsFBK12             TDSSGRILSSAEMYDSETHSWTPLPSMNRARKMCSGVFMDGKFYVVGGV-ASNNKVLTCG
PmF-box1            CDSRGNIRSSAELYDSEKETWEVLPDMIKPRKMCSGVFMDGKFCVIGGIGGSDSKLLTSA
At1g14330           FDSFGKISDSAEMYNSELQTWTTLPKMNKPRKMCSGVFMDGKFYVIGGIGGNDSKVLTCG
At2g20870|SKIP11    CDSQGKILDFAEMYNSELQTWITLPRMNKPRKMCSGVFMDGKFYVIGGIGGADSKGLTCG
                     ** *.* . **:*:** :*  ** * ..************ *:**: . ..* **..


OsFBK12             EEYDLKRRSWRVIENMSE-------------GLNGVTGAPPLIAVVNNELYAADYSEKDV
PmF-box1            EEFDMETRTWKEIPNMSPVGTGPPREN----EMPPSS-APPLVAVVNNELYAADYADMEV
At1g14330           EEFDLETKKWTEIPEMSP-----PRSR----EMPAAAEAPPLVAVVNNELYAADHADMEV
At2g20870|SKIP11    EEYDLETKKWTQIPDLSP-----PRSRADQADMSPAAEAPPLVAVVNNQLYAADHADMEV
                    **:*::  ..*  * ::*      :   : **** :*****:*****::: :*


OsFBK12             KKYDKQNNKWITLGKLPERSVSMNGWGLAFRACGDRLIVIGGPRTSIGGTIELNSWTP--
PmF-box1            RKYNKVTSTWSTVGKLPERAGSMNGWGLAFRGCGDRLIVIGGPRAYGEGVIEVNSWVPND
At1g14330           RKYDKESKKWFTLGRLPERADSVNGWGLAFRACGERLIVIGGPRSSGGGYIELNSWIPSS
At2g20870|SKIP11    RKYDKENKKWLTVGRLPERAGSVNGWGLAFRACGERLIVIGGPKCSGGGFIELNSWIP-S
                    .**:* ...* *:*.****: *:******** **:*.********.    * **.*** *


OsFBK12             DERPPVWNLIARRPSGNFVYNCAVMGC
PmF-box1            D--PPQWTLLARKQLGSFVYNCAVMGC
At1g14330           DRSPPLWTLLGRKHSSNFVYNCAVMGC
At2g20870|SKIP11    DGGPPQWTLLDRKHSPTFVYNCAVMGC
                    *  ** *.*: *.   .**********
```

FIGURE 2. Multiple sequence alignment of *PmF-box1* with its homologs from Arabidopsis and rice

hence, degraded by 26S-proteasome, in systeam known as the ubiquitin 26S-proteasome system (UPS) (Abd-Hamid et al. 2020; Bai et al. 1996).

Two types of transgenic Arabidopsis were generated to characterise the function of *PmF-box1*. First was Arabidopsis overexpressing the full ORF sequence of *PmF-box1*. Second was Arabidopsis overexpressing kelch-modified *PmF-box1* (*KMF*), in which the *KMF* is a sequence with a deleted kelch motif. From previous study, the expression of *PmF-box1* in *P. minor* showed a moderate correlation with the expression of *PmLOX1* (Othman et al. 2017). Through the hydroperoxide lyase (HPL) branch pathway, LOX leads to the formation of green leaf volatiles (GLVs). Analyses were conducted on transgenic Arabidopsis expressing *PmF-box1* and *KMF* to evaluate if the expression of *PmF-box1* altered the generation of GLVs.

The expression of Arabidopsis LOX-HPL branch pathway genes, which are *LOX2* and *HPL* in transgenic Arabidopsis, was plotted in a graph (Figure 3(a)). The optimisation included the construction of qRT-PCR standard curves and melt curve analysis to identify any non-specific amplification of the qRT-PCR products, which were supplied in the supplementary materials (Figure S2 and Figure S3). From the graph in Figure 3(a), the *PmF-box1*-overexpressing Arabidopsis plant has reduced expression of *LOX2* and *HPL* genes compared to other plants. In contrast, the expression of all target genes in the *KMF*-overexpressing Arabidopsis was almost similar to the vector control (VC) plants. These results suggested that the KMF could not function as PmF-box1 because of the loss of kelch-repeat in the sequence.

Compared to our previous study of the plant overexpressing *AtSKIP11/AT2G02780/AtARKP1* (Naeem-Ul-Hassan et al. 2017) as in Figure 3(b) with the *PmF-box1*-overexpressing plant in Figure 3(a), the expression patterns of *LOX2* and *HPL* genes were almost the same. Furthermore, based on the analysis of *skip11* mutant (SALK_019581.24.40.x) plants in our previous study (Naeem-Ul-Hassan et al. 2018), the *LOX2* and *HPL* genes (Figure 3(c)) also showed almost the same expression pattern as in the *AtSKIP11-antisense* plant (Figure 3(b)). Then, for *the KMF*-overexpressing

plant (Figure 3a), the *KMF* sequence did not behave like an *AtSKIP11-antisense* or *skip11* mutant because the endogenous *AtSKIP11* expression was not affected. However, *LOX2* and *HPL* genes still showed higher expression in *the KMF*-overexpressing plant than in the *PmF-box1*-overexpressing plant (Figure 3(a)), in which the pattern was almost similar based on the comparison of the *AtSKIP11-antisense* plant and the *AtSKIP11*-overexpressing plant (Figure 3(b)). Therefore, it was speculated that KMF might still function to interact with Skp1 to form the FBP-Skp1 (KMF-Skp1) subcomplex, which then could influence the abundance of formation of the functional SCF complex, FBP(SKIP11)-Skp1-Cullin-Rbx1 for protein degradation (Abd-Hamid et al. 2020). Nevertheless, the comparison between *PmF-box1*-overexpressing plants and *SKIP11*-overexpressing plants gave some insights that *PmF-box1* could play similar roles as SKIP11 from Arabidopsis.

Until today, the target protein of SKIP11/AT2G02780/AtARKP1 remains unknown. In Arabidopsis, *SKIP11/AT2G02780/AtARKP1* was discovered to interact with Skp1-like protein, which is the main component of the SCF complex (Li et al. 2015; Oughtred et al. 2019; Risseeuw et al. 2003). Li et al. (2015) demonstrated that at the transcriptional level, *SKIP11/AT2G02780/AtARKP1* acts as a positive regulator under drought stress conditions, where it was hypothesised to play a decisive function in the network of ABA signalling. Transgenic Arabidopsis of *ARKP1*-overexpressing exhibited elevated expression of ABA and drought-responsive marker genes (*RAB18, AB12, RD29A* and *ABF3*) in comparison to wild-type and *arkp1* mutant (SALK_078824) plants. In contrast, the phenotype of the *arkp1* mutant exhibited reduced sensitivity to the action of ABA and reduced drought tolerance.

In rice, Chen et al. (2013) found that OsFBK12, the homolog of *SKIP11/AT2G02780/AtARKP1* and *PmF-box1*, interacts with S-adenosyl-L-methionine synthetase1 (SAMS1). The interaction between OsFBK12 and OSK1, an Skp1-like protein from rice, was also validated. The regulation of SAMS1 degradation through UPS mediated by OsFBK12 function in the SCF complex was also reported through the analysis of protein degradation assays. In plant metabolism, SAMS (EC 2.5.1.6) is a critical enzyme in ethylene biosynthesis. SAMS catalyses S-adenosyl-L-methionine (SAM) biosynthesis, a precursor for ethylene biosynthesis from methionine and ATP (Wang et al. 2002; Yang & Hoffman 1984).
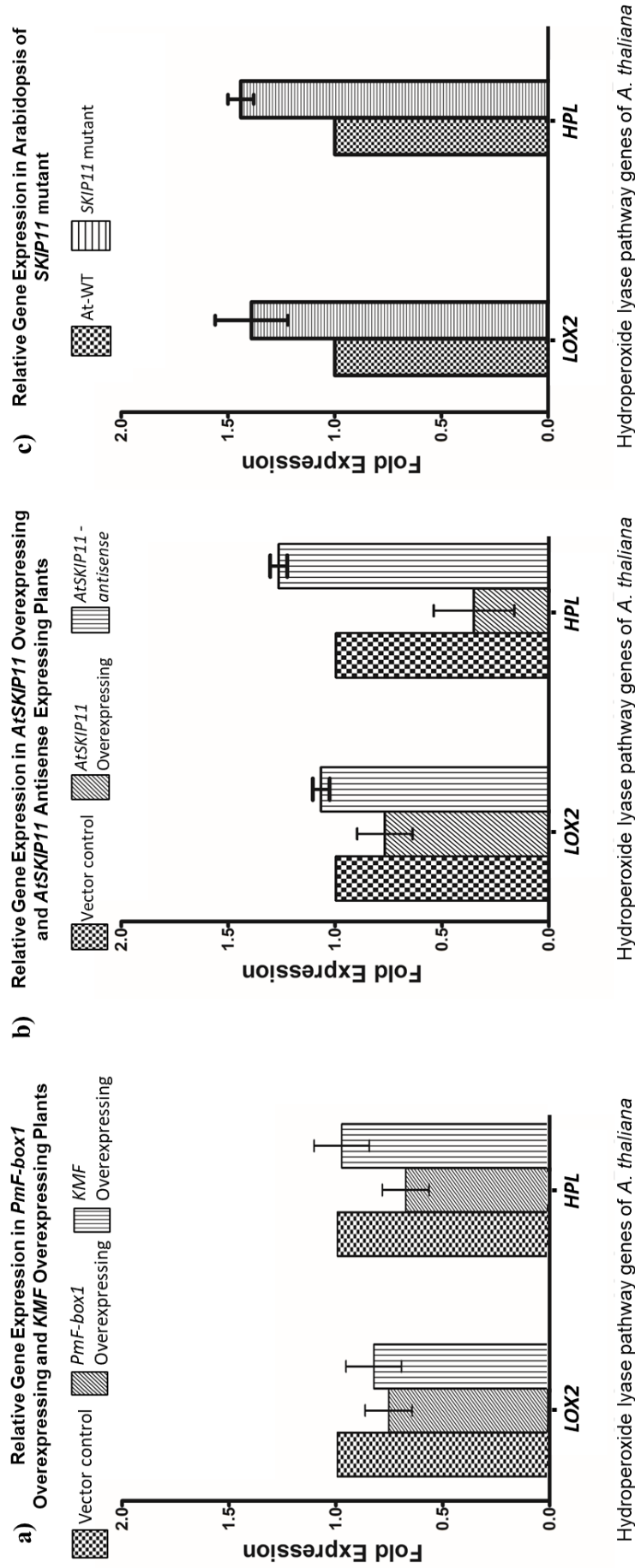
a) Relative Gene Expression in *PmF-box1* Overexpressing and *KMF* Overexpressing Plants

Hydroperoxide lyase pathway genes of *A. thaliana*

b) Relative Gene Expression in *AtSKIP11* Overexpressing and *AtSKIP11* Antisense Expressing Plants

Hydroperoxide lyase pathway genes of *A. thaliana*

c) Relative Gene Expression in Arabidopsis of *SKIP11* mutant

Hydroperoxide lyase pathway genes of *A. thaliana*

FIGURE 3. Graphical presentation of the changes in the expression levels of the LOX-HPL pathway genes. a) Overexpression of *PmF-box1* and overexpression of *KMF* in Arabidopsis. b) Overexpression of *AtSKIP11* and *AtSKIP11* antisense in Arabidopsis adapted from Naeem-Ul-Hassan et al. (2017). c) Expression comparison in WT and *AtSKIP11* mutant adapted from Naeem-Ul-Hassan et al. (2018)

Chen et al. (2013) also reported that the overexpression of OsFBK12 lowered seed germination while RNAi-OsFBK12 increased seed germination. The production of ACC and ethylene in the transgenic plants was also parallel with the seed germination results. In addition, research on *SKIP11/AT2G02780/AtARKP1* in Arabidopsis also showed its negative effect on seed germination (Li et al. 2015). According to both studies, the expression of *SKIP11/AT2G02780/AtARKP1* negatively affects seed germination. Based on the sequence similarities and parallel results of seed germination assay from both research, it is suggested that SAMS is a potential target protein that interacts *with SKIP11/AT2G02780/AtARKP1* in Arabidopsis and also for *PmF-box1* from *P. minor*. From the analysis, it is positively shown that ethylene plays a critical role in releasing seed dormancy. In addition, it is known that ethylene has an antagonistic effect on ABA in seed germination, as Ghassemian et al. (2000) showed that ethylene influences lowered seed germination in the presence of ABA. According to another research,

ethylene can affect the transcriptional level of LOX-HPL pathway genes, hence positively influencing the gene expression of aroma volatile-related enzymes, *LOX*, *HPL* and ADH in fruits (Li et al. 2016; Xie et al. 2011; Yang et al. 2016). These studies provide additional evidence that SAMS may be the potential target protein for *SKIP11/AT2G02780/AtARKP1* and *PmF-box1* (Figure 4).

GLV PRODUCTION IN THE TRANSGENIC ARABIDOPSIS

To further analyse the transgenic Arabidopsis, HS-SPME-GCMS was used to determine the changes in the GLV level of the *PmF-box1*-overexpressing and the *KMF*-overexpressing plants to compare with the VC plants. A representative chromatogram and four concentration points on the standard curve for Z-3-hexen-1-ol are shown. The first alcoholic GLV synthesised in the LOX-HPL pathway was constructed to determine its levels quantitatively (supplementary material, Figures S4 and S5). The GCMS chromatograms produced well-resolved peaks for various GLVs with similar patterns
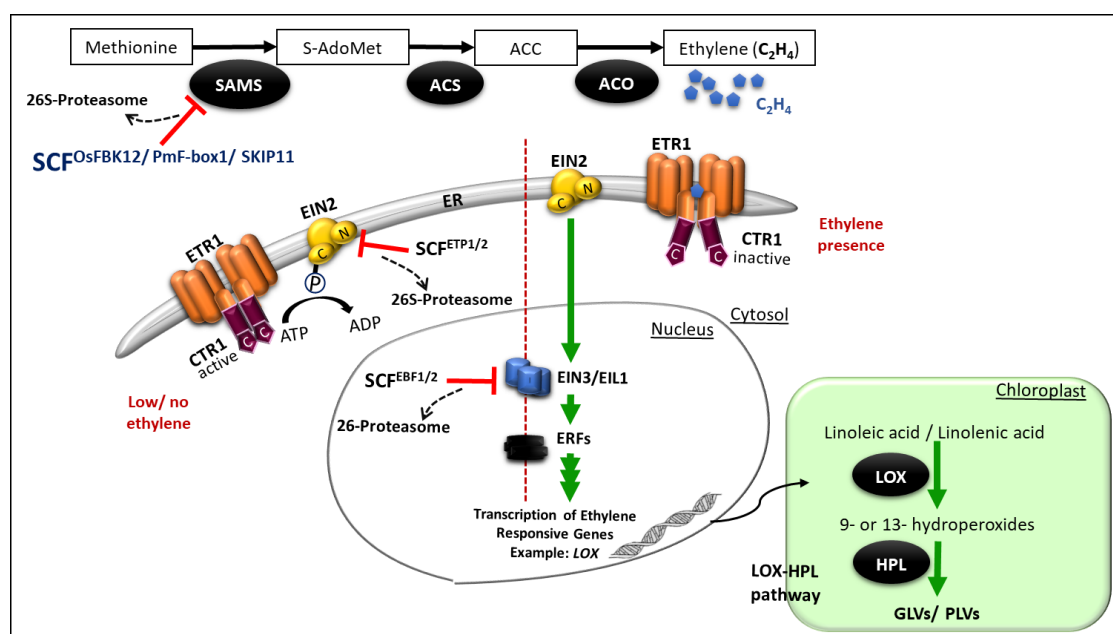
FIGURE 4. Illustration of the action of *PmF-box1* which indirectly affects GLV/ PLV production. GLVs and PLVs were affected when the ethylene biosynthesis was interrupted. In the ethylene biosynthesis, SAMS is suggested to be regulated by *PmF-box1* that form the SCF complex and participates in the UPS for protein degradation. The left side is a condition with low ethylene where EIN2 and EIN3/EIL1 will be degraded through UPS mediated by the SCF complex. The right side is a condition where ethylene signalling occurs. SAMS (S-adenosyl methionine synthetase), S-AdoMet (S-adenosyl-L-methionine), ACC (1-aminocyclopropane-1-carboxylic acid), ACS (ACC synthase), ACO (ACC oxidase), LOX (Lipoxygenase), HPL (hydroperoxide lyase), ER (endoplasmic reticulum), ETR1 (ethylene receptor 1), CTR1 (constitutive triple response 1 (kinase protein)), EIN2 (ethylene-insensitive 2), EIN3/EIL (ethylene-insensitive 3/ EIN3-like), ERF (ethylene response factor), GLVs (green leaf volatiles) and PLVs (five-carbon pentyl leaf volatiles)

(supplementary material, Figure S6 to S8), where the chromatograms showed volatile organic compounds, including several GLVs. However, only four volatile compounds were selected for comparison of their levels of emission by different transgenic plants. The volatile compounds included hexanal, 1-hexanol and (Z)-3-hexen-1-ol, which are C6 GLVs, and the C5 volatile, 1-penten-3-ol because those compounds were detected in measurable amounts in all the transgenic and control plants used in this study. Hexanal, 1-hexanol, (Z)-3-hexen-1-ol and 1-penten-3-ol were quantified by averaging the mass abundance of each compound per gram of fresh leaf material from the respective chromatograms, and the relative standard deviation (RSD) was determined (supplementary material, Table S1). Along with their retention times, the average mass abundance values of each compound in transgenic and control plants were listed in Table 4.

In order to compare the volatile compounds produced by transgenic plants and VC plants, the quantities of C6 and C5 compounds per gram of fresh leaf material and corresponding RSD values were presented in Figure 5. This research demonstrated a significant decrease in the production of hexanal, 1-hexanol, (Z)-3-hexen-1-ol, and 1-penten-3-ol in *KMF*-overexpressing plants compared to VC plants. Then, for *PmF-box1*-overexpressing plants, hexanal was the only compound that showed a significant reduction compared to VC plants. In contrast, the comparison between *PmF-box1*-overexpressing plants and *KMF*-overexpressing plants showed that two GLVs, 1-hexanol and (Z)-3-hexen-1-ol, were significantly lower in *KMF*-overexpressing plants. The concentrations of (Z)-3-hexen-1-ol, the most important GLV in this research, emitted by the VC plants

were calculated from the standard curve equation given in the supplementary material (Figure S5) and found to be 238.04 nM per gram of the fresh leaf material. In comparison, the computed values for the transgenic plants overexpressing *PmF-box1* and *KMF* were 240 nM and 109.62 nM, respectively. The maximum concentration of (Z)-3-hexenal, (E)-2-hexenal and (Z)-3-hexenol emitted by fully injured tissue was determined to be 496 nM GLVs per gram of the fresh weight in *A. thaliana* (Shiojiri et al. 2012).

The analysis of transgenic Arabidopsis plants with overexpressed *PmF-box1* and *KMF* showed that the genes influence the LOX-HPL pathway. In the *PmF-box1* overexpressing plant, the production of GLVs was relatively parallel to the expression of the LOX-HPL branch genes, particularly in the production of hexanal and 1-penten-3-ol. Lower hexanal production in both transgenic plants correlated with *LOX* expression, where decreased *LOX* expression might result in lower LOX activity and, hence, lower hexanal production. There were no significant differences between the *PmF-box1*-overexpressing plant and the control plant regarding the generation of C6 alcohols. ADH1 catalyses the synthesis of C6 alcohols from their corresponding aldehydes. However, the expression of *ADH1* was not examined in this study. According to Salas et al. (2006), ADH activity appears to vary even across individual WT Arabidopsis. In another kingdom, Drosophila also shows that *ADH* expression is not reflected in ADH activity (Malherbe et al. 2005).

In the past six years, a *LOX2* gene from *Arabidopsis* has been identified to play a crucial role in GLVs and C5 volatiles biosynthesis (Mochizuki et al. 2016). In another research, TomloxC, a 13-LOX from

TABLE 4. Retention times and the abundance (arbitrary units) of distinct GLVs

GLVs	RT (min.)	Vector Control (VC)	*PmF-box1* overexpressing	*KMF* overexpressing
Hexanal	4.81	116,626,720	60,716,487	40,182,852
1-Penten-3-ol	7.60	259,950,250	183,358,771	108,318,911
1-Hexanol	13.42	63,358,315	75,263,642	40,614,402
(Z)-3-Hexen-1-ol	14.27	266,519,968	268,385,077	144,311,395

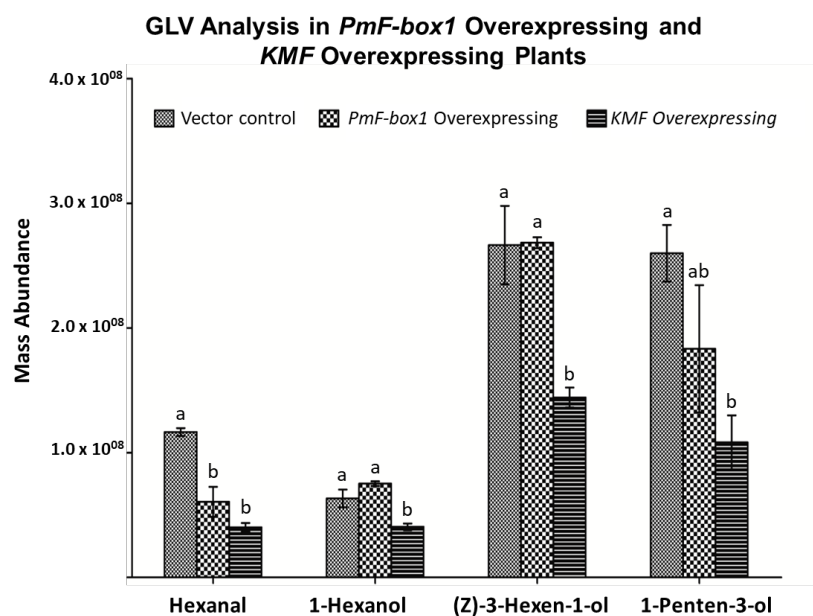## GLV Analysis in *PmF-box1* Overexpressing and *KMF* Overexpressing Plants

FIGURE 5. The relative abundance (arbitrary units) of different GLVs per grams of fresh leaf material in transgenic and vector control plants. Tukey's HSD test was run at a p-value < 0.05. The letters above the bars show the significant difference between GLVs compared to different transgenic plants

tomato, has been elucidated in the production of C5 volatiles (Shen et al. 2014). Based on suppression analysis of the *HPL* gene, analysis of *lox2* mutant Arabidopsis showed the importance of LOX2 in regulating GLVs production, which is independent of HPL activity (Mochizuki et al. 2016). He et al. (2020) showed in a separate study that *LOX10* from *Zea mays* could also catalyse the biosynthesis of PLVs apart from GLVs. Previous research on the suppression of *LOX* and *HPL* in potatoes discovered that these compounds significantly influenced the production of C6 and C5 leaf volatiles (Salas et al. 2005). The suppression of *HPL* resulted in a considerable increase in LOX activity and C5 volatiles. Then, Salas et al. (2006) study in Arabidopsis also suggested that an increment in the LOX activity in the *hpl* mutant is responsible for the decrease of C6 GLVs and high formation of C5 PLVs. The formation of high PLVs production is suggested to be generated from the homolytic cleavage of 13-hydroperoxides by LOX (Gorman et al. 2021; Salas et al. 2006, 2005; Salch et al. 1995; Shen et al. 2014). Observation on the relative proportion of 1-penten-3-ol to hexanal production in VC is 2.23, while in *PmF-box1* and *KMF*-overexpressing plants were 3.02

and 2.70, respectively. From this observation, the increased relative proportion of 1-penten-3-ol to hexanal production might be due to the lower HPL activity in the *PmF-box1*-overexpressing plant, which might be related to the lower *HPL* transcript level.

CONCLUSION

These data indicated that the changes identified in the gene expression levels, especially GLV formation in the transgenic plants, were due to SCF$^{PmF-box1}$. These changes may be attributed to the interactions of the two kelch-repeats that are part of the *PmF-box1* protein structure with some selective proteins in *A. thaliana*. Based on the sequence similarity of *PmF-box1* with OsFBK12, SAMS1 was the highest possible targeted protein of *PmF-box1* and its homolog in Arabidopsis, which was *SKIP11/AT2G02780/AtARKP1*. It is recommended here that the changes in the GLVs production are not due to the direct interaction of SCF$^{PmF-box1}$ with the proteins or transcription factors involved in the LOX-HPL pathway. Nevertheless, it is due to the interaction with SAMS1, which is the critical enzyme in ethylene biosynthesis. Since ethylene can positively affect the expression of

LOX, *HPL* and *ADH* (Li et al. 2016; Xie et al. 2011; Yang et al. 2016), overexpression of *PmF-box1* in the plant can reduce ethylene production and hence decrease the expression of LOX-HPL pathway genes. This suggestion complemented the analysis of the *skip11* mutant (SALK_019581.24.40.x) plant, which demonstrates that *SKIP11* negatively regulates the production of GLVs and PLVs (Figure 4).

REFERENCES

Abd-Hamid, N.A., Ahmad-Fauzi, M.I., Zainal, Z. & Ismail, I. 2020. Diverse and dynamic roles of F-box proteins in plant biology. *Planta* 251(3): 68.

Bai, C., Sen, P., Hofmann, K., Ma, L., Goebl, M., Harper, J.W. & Elledge, S.J. 1996. *SKP1* connects cell cycle regulators to the ubiquitin proteolysis machinery through a novel motif, the F-box. *Cell* 86: 263-274.

Chen, Y., Xu, Y., Luo, W., Li, W., Chen, N., Zhang, D. & Chong, K. 2013. The F-box protein OsFBK12 targets OsSAMS1 for degradation and affects pleiotropic phenotypes, including leaf senescence, in rice. *Plant Physiology* 163(4): 1673-1685.

Christapher, P.V., Parasuraman, S., Christina, J.M., Asmawi, M.Z. & Vikneswaran, M. 2015. Review on *Polygonum minus* Huds., a commonly used food additive in Southeast Asia. *Pharmacognosy Research* 7(1): 1-6.

Clough, S.J. & Bent, A.F. 1998. Floral dip: A simplified method for *Agrobacterium*-mediated transformation of *Arabidopsis thaliana*. *Plant Journal* 16(6): 735-743.

Engelberth, J., Alborn, H.T., Schmelz, E.A. & Tumlinson, J.H. 2004. Airborne signals prime plants against insect herbivore attack. *Proceedings of the National Academy of Sciences* 101(6): 1781-1785.

Engelberth, J., Contreras, C.F., Dalvi, C., Li, T. & Engelberth, M. 2013. Early transcriptome analyses of Z-3-hexenol-treated *Zea mays* revealed distinct transcriptional networks and anti-herbivore defense potential of green leaf volatiles. *PLoS ONE* 8(10): e77465.

Feng, Z., Mao, Y., Xu, N., Zhang, B., Wei, P., Yang, D.L., Wang, Z., Zhang, Z., Zheng, R., Yang, L., Zeng, L., Liu, X. & Zhu, J.K. 2014. Multigeneration analysis reveals the inheritance, specificity, and patterns of CRISPR/Cas-induced gene modifications in *Arabidopsis*. *Proceedings of the National Academy of Sciences of the United States of America* 111(12): 4632-4637.

Gershenzon, J. 2007. Plant volatiles carry both public and private messages. *Proceedings of the National Academy of Sciences of the United States of America* 104(13): 5257-5258.

Ghassemian, M., Nambara, E., Cutler, S., Kawaide, H., Kamiya, Y. & Mccourt, P. 2000. Regulation of abscisic acid signaling by the ethylene response pathway in arabidopsis. *The Plant Cell* 12(7): 1117-1126.

Gor, M.C., Ismail, I., Mustapha, W.a.W., Zainal, Z., Noor, N.M., Othman, R. & Hussein, Z.a.M. 2010. Identification of cDNAs for jasmonic acid-responsive genes in *Polygonum minus* roots by suppression subtractive hybridization. *Acta Physiologiae Plantarum* 33(2): 283-294.

Gorman, Z., Tolley, J.P., Koiwa, H. & Kolomiets, M.V. 2021. The synthesis of pentyl leaf volatiles and their role in resistance to anthracnose leaf blight. *Frontiers in Plant Science* 12: 719587.

He, Y., Borrego, E.J., Gorman, Z., Huang, P.C. & Kolomiets, M.V. 2020. Relative contribution of LOX10, green leaf volatiles and JA to wound-induced local and systemic oxylipin and hormone signature in *Zea mays* (maize). *Phytochemistry* 174: 112334.

Li, Y., Liu, Z., Wang, J., Li, X. & Yang, Y. 2015. The Arabidopsis Kelch repeat F-box E3 ligase ARKP1 plays a positive role for the regulation of abscisic acid signaling. *Plant Molecular Biology Reporter* 34(3): 582-591.

Li, Y., Qi, H., Jin, Y., Tian, X., Sui, L. & Qiu, Y. 2016. Role of ethylene in the biosynthetic pathway of related-aroma volatiles derived from fatty acids in oriental sweet melon. *Journal of the American Society for Horticultural Science* 141(4): 327-338.

Malherbe, Y., Kamping, A., Delden, W.V. & Zande, L.V.D. 2005. ADH enzyme activity and *Adh* gene expression in *Drosophila melanogaster* lines differentially selected for increased alcohol tolerance. *Journal of Evolutionary Biology* 18(4): 811-819.

Mochizuki, S., Sugimoto, K., Koeduka, T. & Matsui, K. 2016. Arabidopsis lipoxygenase 2 is essential for formation of green leaf volatiles and five-carbon volatiles. *FEBS Letters* 590(7): 1017-1027.

Naeem-Ul-Hassan, M., Zainal, Z. & Ismail, I. 2015. Green leaf volatiles: biosynthesis, biological functions and their applications in biotechnology. *Plant Biotechnology Journal* 13(6): 727-739.

Naeem-Ul-Hassan, M., Zainal, Z., Abd Hamid, N.A., Sajad, M. & Ismail, I. 2018. Arabidopsis *AT2G02870* loss of function mutants lead to enhanced production of hydroperoxide lyase pathway genes and products. *Sains Malaysiana* 47(12): 3003-3008.

Naeem-Ul-Hassan, M., Zainal, Z., Kiat, C.J., Monfared, H.H. & Ismail, I. 2017. *Arabidopsis thaliana* SKP1 interacting protein 11 (At2g02870) negatively regulates the release of green leaf volatiles. *RSC Advances* 7(88): 55725-55733.

Othman, M.H.C., Hadi, N.A., Zainal, Z., Kiat, C.J., Naeem-Ul-Hassan, M., Zain, C.R.C.M. & Ismail, I. 2017. Expression profile of gene encoding Kelch repeat containing F-box protein (*PmF-box1*) in relation to the production of green leaf volatiles. *Australian Journal of Crop Science* 11(04): 406-418.

Oughtred, R., Stark, C., Breitkreutz, B.J., Rust, J., Boucher, L., Chang, C., Kolas, N., O'donnell, L., Leung, G., Mcadam, R., Zhang, F., Dolma, S., Willems, A., Coulombe-Huntington, J., Chatr-Aryamontri, A., Dolinski, K. & Tyers, M. 2019. The BioGRID interaction database: 2019 update. *Nucleic Acids Research* 47(D1): D529-D541.

Risseeuw, E., Daskalchuk, T., Banks, T., Liu, E., Cotelesage, J., Hellmann, H., Estelle, M., Somers, D. & Crosby, W. 2003. Protein interaction analysis of SCF ubiquitin E3 ligase subunits from *Arabidopsis*. *The Plant Journal* 34(6): 753-767.

Salas, J.J., Garcia-Gonzalez, D.L. & Aparicio, R. 2006. Volatile compound biosynthesis by green leaves from an *Arabidopsis thaliana* hydroperoxide lyase knockout mutant. *Journal of Agricultural and Food Chemistry* 54(21): 8199-8205.

Salas, J.J., Sanchez, C., Garcia-Gonzalez, D.L. & Aparicio, R. 2005. Impact of the suppression of lipoxygenase and hydroperoxide lyase on the quality of the green odor in green leaves. *Journal of Agricultural and Food Chemistry* 53(5): 1648-1655.

Salch, Y.P., Grove, M.J., Takamura, H. & Gardner, H.W. 1995. Characterization of a C-5,13-cleaving enzyme of 13(S)-hydroperoxide of linolenic acid by soybean seed. *Plant Physiology* 108(3): 1211-1218.

Sarang, K., Rudziński, K.J. & Szmigielski, R. 2021. Green leaf volatiles in the atmosphere - properties, transformation, and significance. *Atmosphere* 12(12): 1655.

Shen, J., Tieman, D., Jones, J.B., Taylor, M.G., Schmelz, E., Huffaker, A., Bies, D., Chen, K. & Klee, H.J. 2014. A 13-lipoxygenase, TomloxC, is essential for synthesis of C5 flavour volatiles in tomato. *Journal of Experimental Botany* 65(2): 419-428.

Shiojiri, K., Ozawa, R., Matsui, K., Sabelis, M.W. & Takabayashi, J. 2012. Intermittent exposure to traces of green leaf volatiles triggers a plant response. *Scientific Reports* 2: 378.

Vikram, P., Chiruvella, K.K., Ripain, I.H. & Arifullah, M. 2014. A recent review on phytochemical constituents and medicinal properties of kesum (*Polygonum minus* Huds.). *Asian Pacific Journal of Tropical Biomedicine* 4(6): 430-435.

Vincenti, S., Mariani, M., Alberti, J.-C., Jacopini, S., Brunini-Bronzini De Caraffa, V., Berti, L. & Maury, J. 2019. Biocatalytic synthesis of natural green leaf volatiles using the lipoxygenase metabolic pathway. *Catalysts* 9(10): 873.

Wang, K.L., Li, H. & Ecker, J.R. 2002. Ethylene biosynthesis and signaling networks. *Plant Cell* 14: S131-S151.

Wang, Y., Suo, H., Zhuang, C., Ma, H. & Yan, X. 2011. Overexpression of the soybean *GmWNK1* altered the sensitivity to salt and osmotic stress in *Arabidopsis*. *Journal of Plant Physiology* 168(18): 2260-2267.

Xie, Y.H., Gao, H.Y., Luo, Y.B., Zhang, H.X., Chen, X.N. & Zhu, B.Z. 2011. Role of ethylene in the biosynthesis of fatty acid-derived volatiles in tomato fruits. *Advanced Materials Research* 343-344: 937-950.

Yang, S.F. & Hoffman, N.E. 1984. Ethylene biosynthesis and its regulation in higher plants. *Annual Review of Plant Physiology* 35: 155-189.

Yang, X., Song, J., Du, L., Forney, C., Campbell-Palmer, L., Fillmore, S., Wismer, P. & Zhang, Z. 2016. Ethylene and 1-MCP regulate major volatile biosynthetic pathways in apple fruit. *Food Chemistry* 194: 325-336.

Zhang, X., Gou, M. & Liu, C.J. 2013. Arabidopsis Kelch repeat F-box proteins regulate phenylpropanoid biosynthesis via controlling the turnover of phenylalanine ammonia-lyase. *The Plant Cell* 25(12): 4994-5010.

***Corresponding author; email: maniz@ukm.edu.my

SUPPLEMENTARY MATERIALS
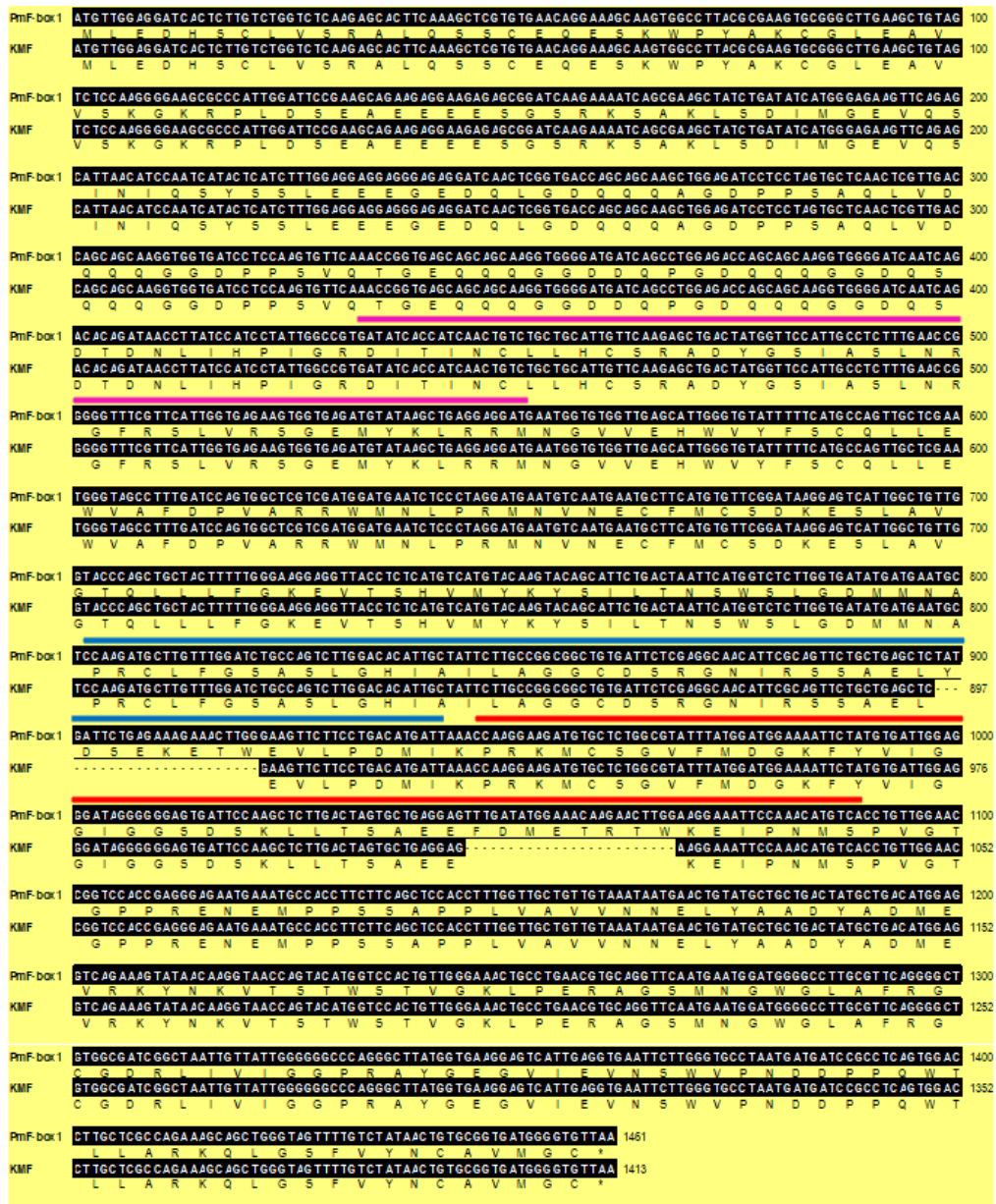
FIGURE S1. Sequence alignment between *PmF-box1* and kelch modified *PmF-box1* (*KMF*). There are 24 bps in the kelch 1 and kelch 2 region were deleted on the *KMF* sequence
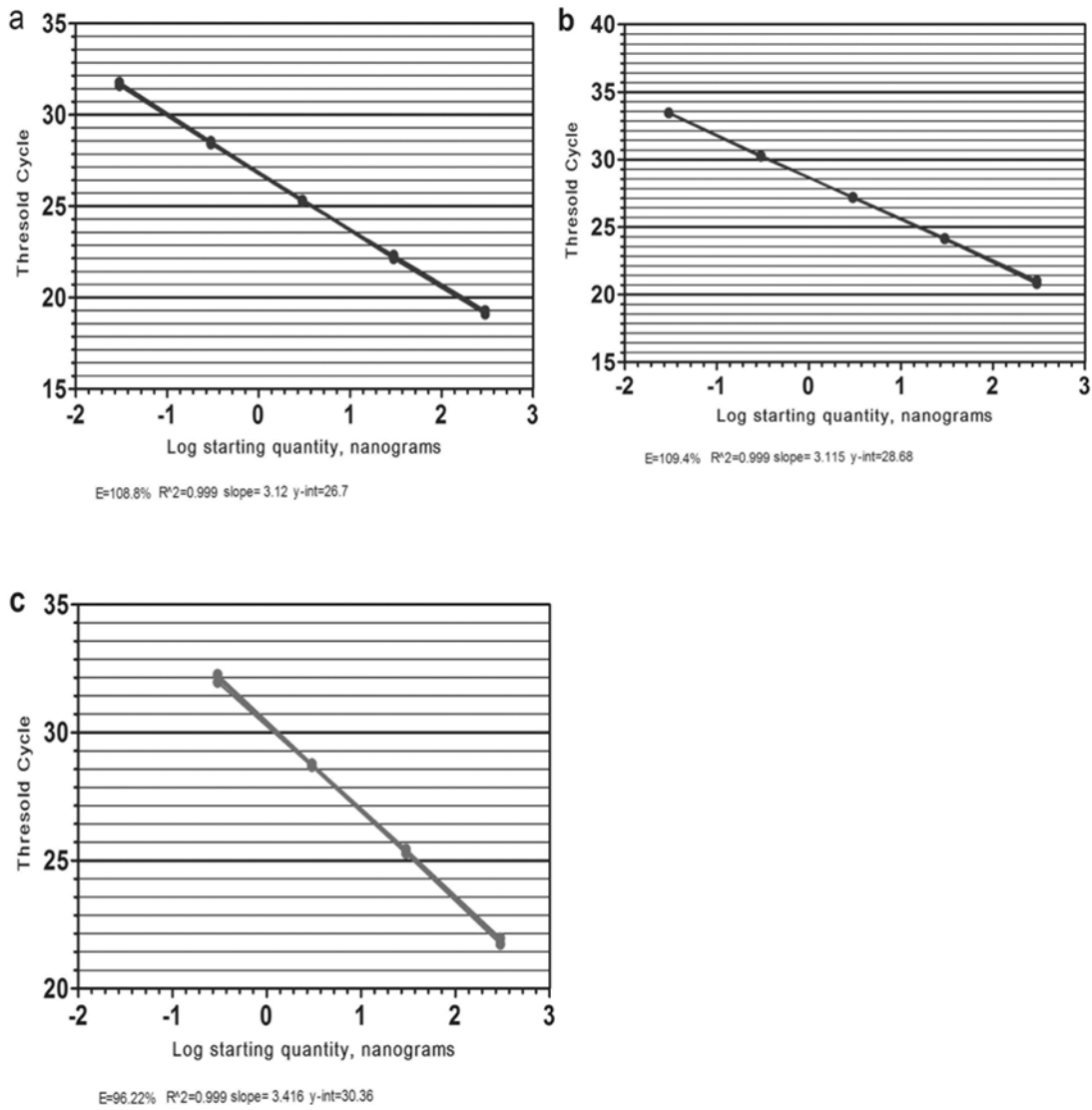
FIGURE S2. Standard curves for the *Actin-2*, *LOX2* and *HPL* genes (a – c respectively). Calibration curves were constructed for optimization of various parameters, such as the template and primers concentration to achieve a reliable comparison among the samples and the controls. Using the control samples cDNA as the template, 10-fold dilution factor for five or four dilution points were plotted against the respective CT values to determine the efficiency, R^2 and the slope
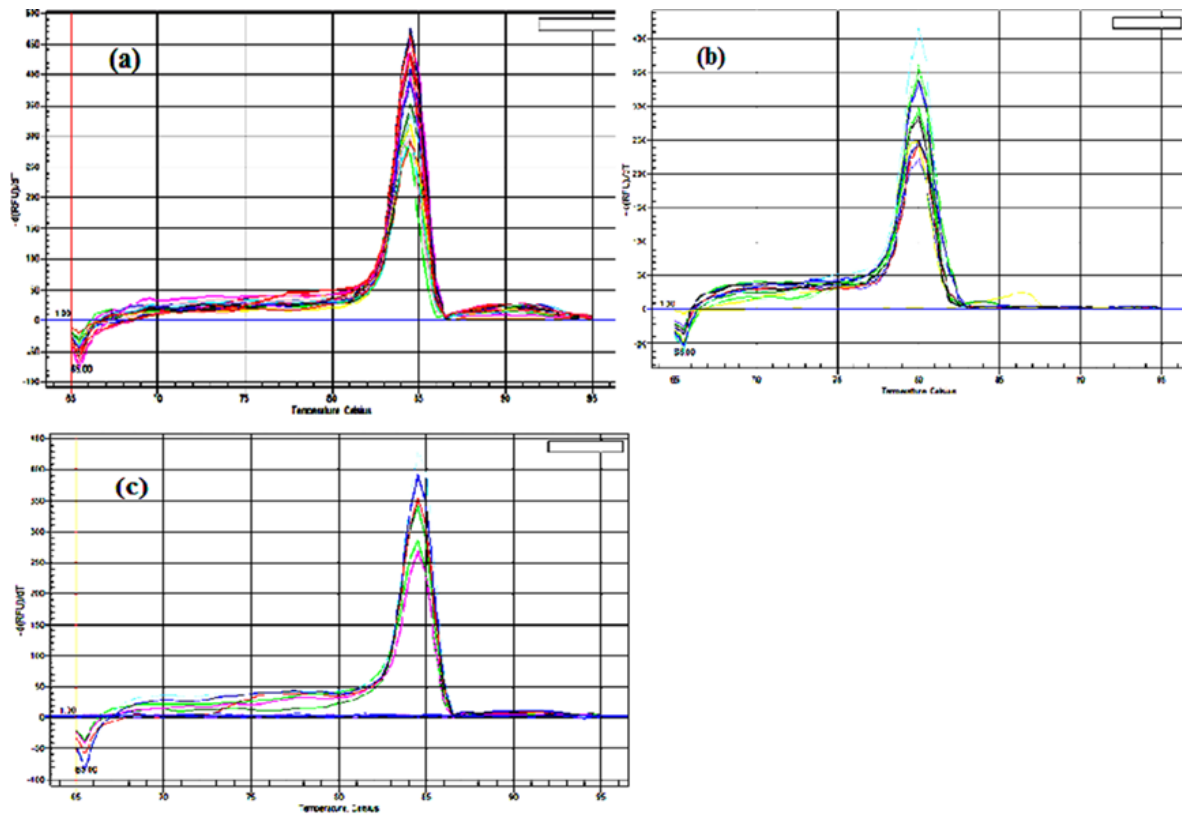
FIGURE S3. Melt curve graphs from RT-qPCR analysis. (a) Actin-2, (b) LOX-2 and (c) HPL. Different reaction products, including the non-specific products in the qRT-PCR can be identified by the melt curve analysis following the amplification reaction. This is done by raising the temperature in small increments and monitoring the emission of fluorescent signal from each step. Denaturation of the double stranded DNA decreases the fluorescence signal. Plotting the negative first derivative of change in fluorescent signal as a function of temperature will yield a characteristic peak at the melting temperature of the amplicon. The non-specific reaction products, including the primer-dimers can be distinguished from the amplicon, as they melt at a different temperature
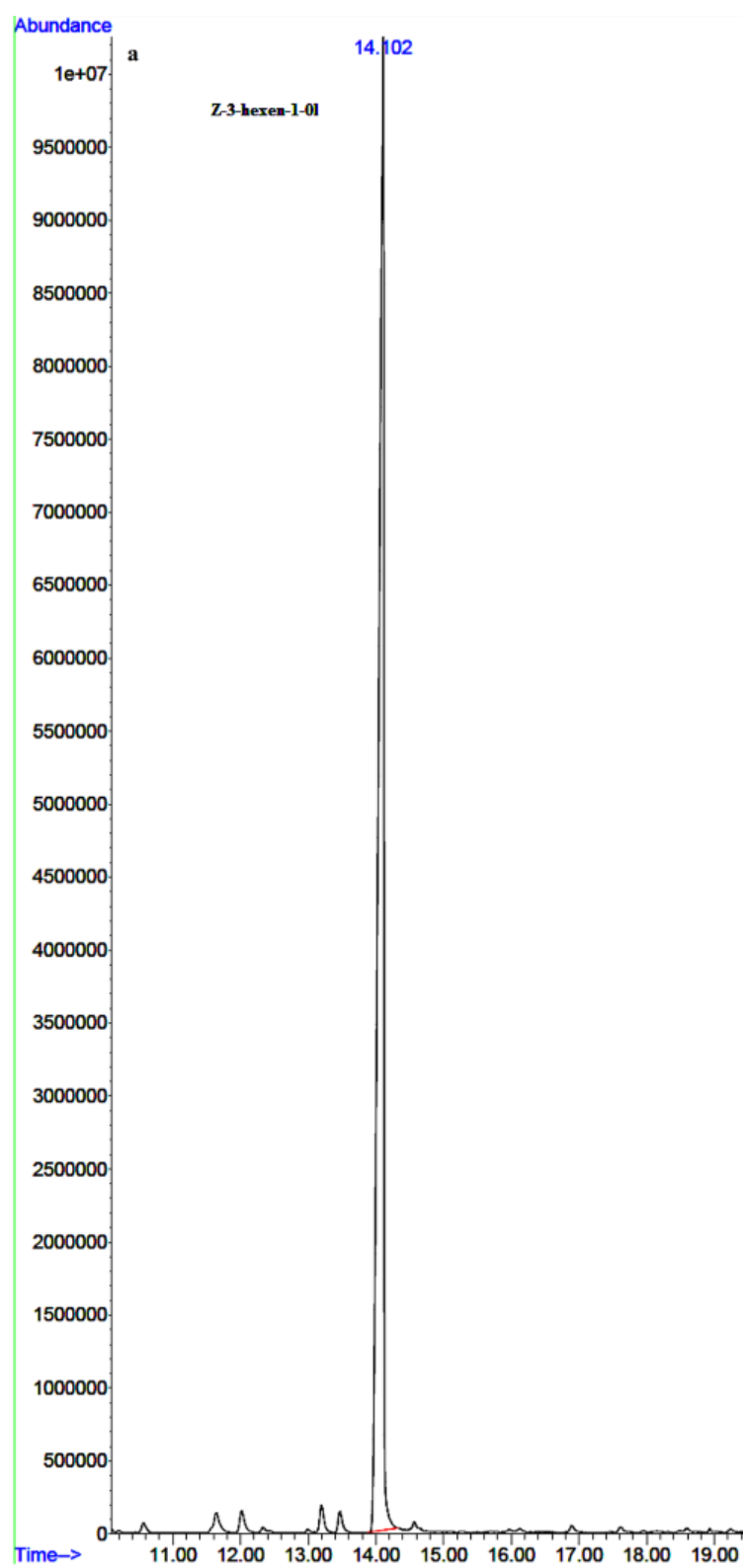
FIGURE S4. GC-MS chromatogram for Z-3-hexen-1-ol standard solution with
500 nM concentration
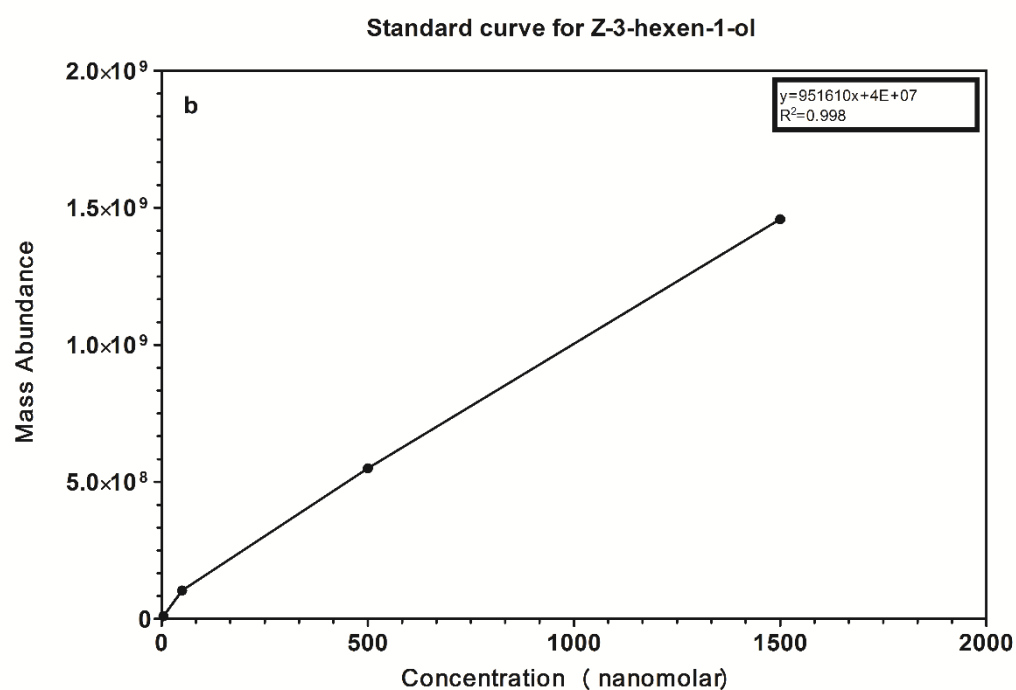
Standard curve for Z-3-hexen-1-ol

FIGURE S5. Standard curve for Z-3-hexen-1-ol. Z-3-hexen-1-ol was chosen for the analysis of HPL pathway because it is the first C6 alcohol produced in the pathway by the sequential actions of the LOX, HPL and ADH enzymes. Four concentration points at 5, 50, 500, and 1500 nanomolar (nM) were used to produce a standard curve for Z-3-hexen-1-ol. Plotting the mass abundance of Z-3-hexen-1-ol, obtained by SPME-GC-MS chromatograms, against the concentration at each point yield a straight line with R^2 value of 0.998. The concentration of Z-3-hexen-1-ol, formed in different plant samples was calculated using the equation derived from the calibration curve graph, $y = 951610x + 4E^{+07}$
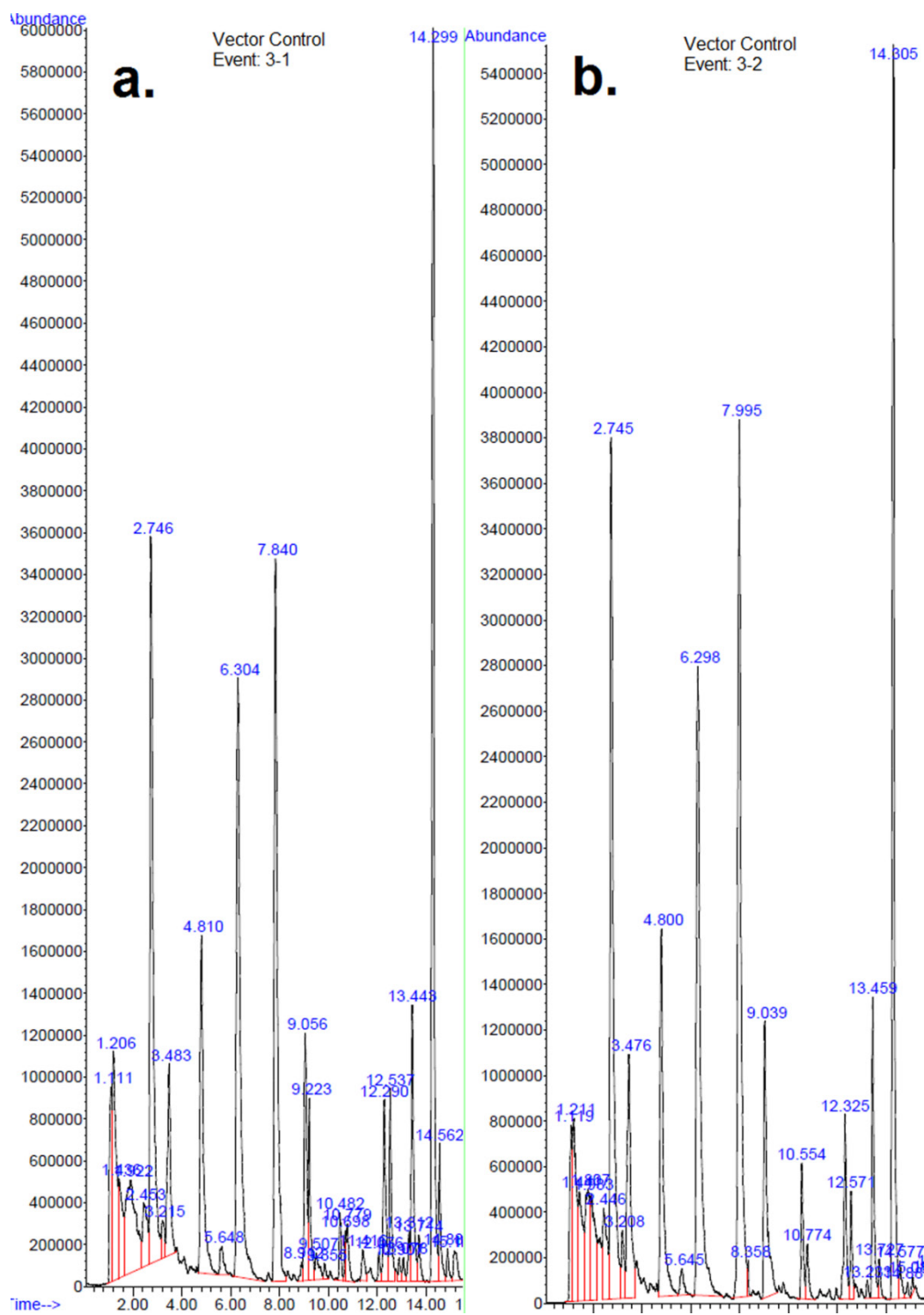
FIGURE S6. GC-MS chromatograms of GLV extracted by HS-SPME from *A. thaliana* control plants with empty vector (a. event 1, b. event 2)
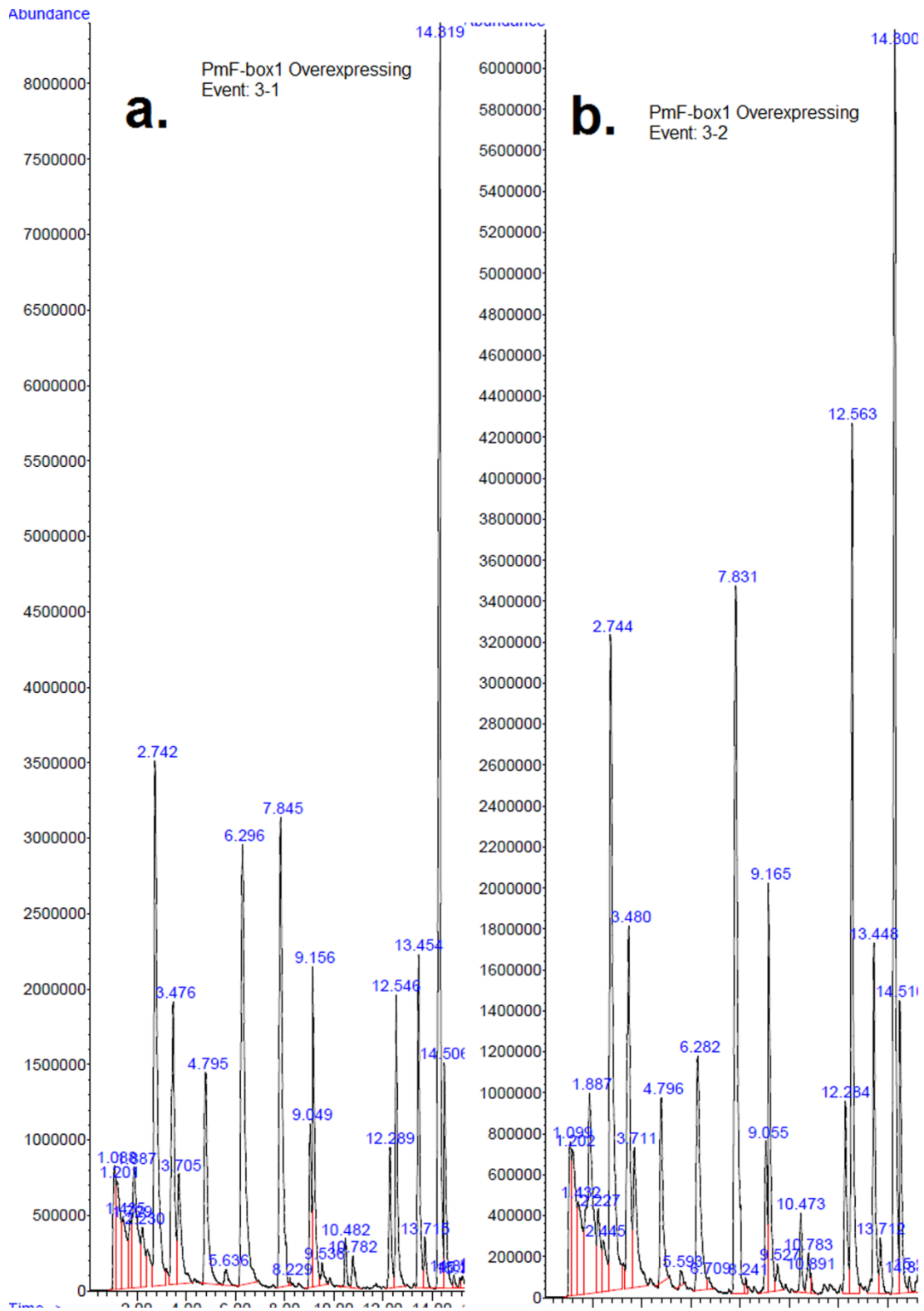
FIGURE S7. GC-MS chromatograms of GLV extracted by HS-SPME from transgenic
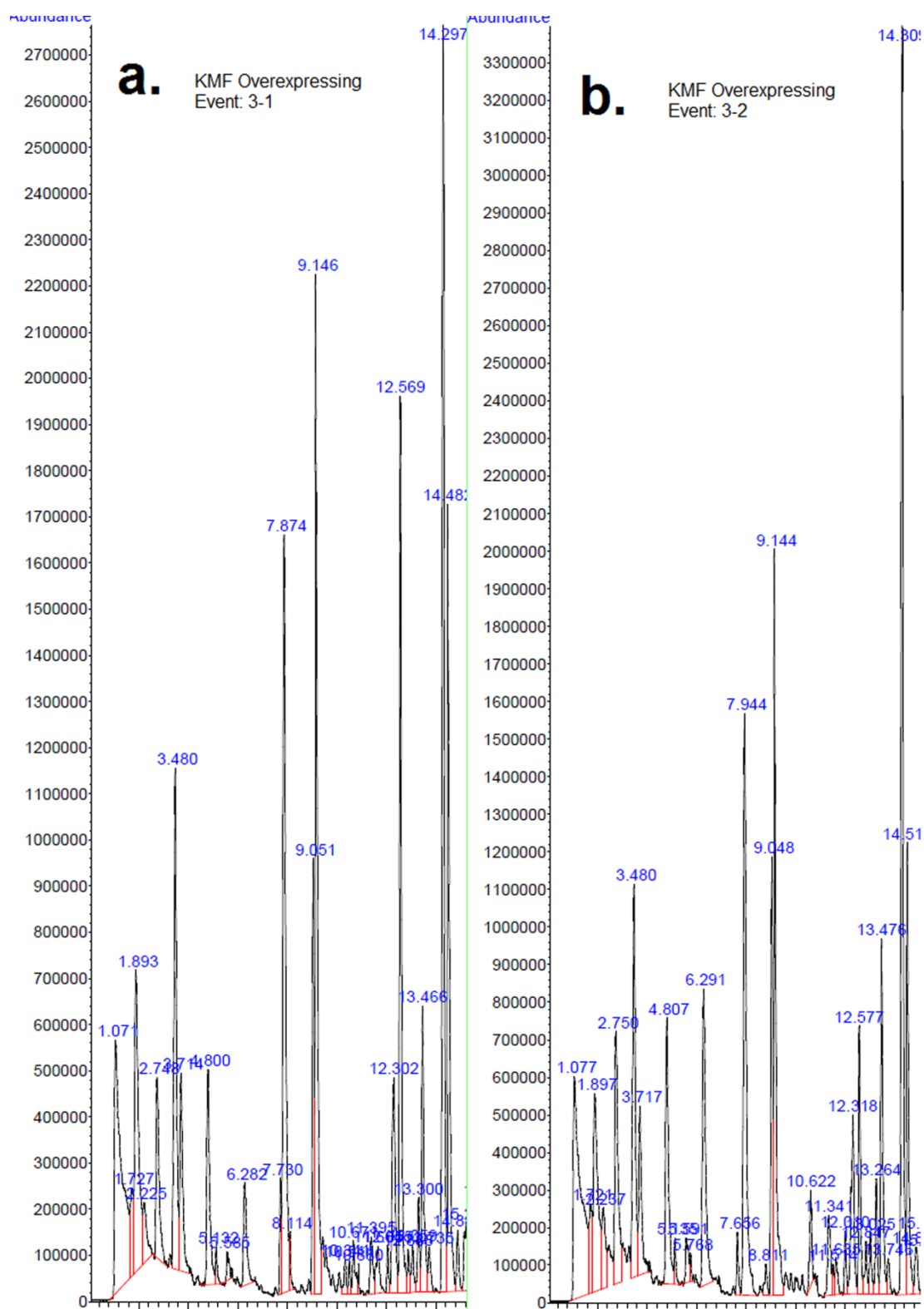*A. thaliana* plants overexpressing *PmF-box1* gene (a. event 1, b. event 2)

FIGURE S8. GC-MS chromatograms of GLV extracted by HS-SPME from *KMF* sequence overexpressing *A. thaliana* plants (a. event 1, b. event 2)

TABLE S1. GLVs calculation from SPME-GC-MS results. Mass abundance of each replicate, average mass abundance and relative standard deviation (RSD) values of different GLV for each type of plants (XP- *PmF-box1* overexpressing and XK- *KMF* sequence overexpressing)

GLV	Sample	Replicate 1	Replicate 2	Average	RSD
Hexanal	Vector Control	118826066	114427374	116626720	3
	XP Plants	69184783	52248191	60716487	20
	XK Plants	37716396	42649307	40182852	9
1-Penten-3-ol	Vector Control	243842072	276058427	259950250	9
	XP Plants	147270317	219447225	183358771	28
	XK Plants	123649650	92988173	108318911	20
1-Hexanol	Vector Control	68344094	58372537	63358315	11
	XP Plants	73924402	76602882	75263642	3
	XK Plants	38721383	42507420	40614402	7
(Z)-3-Hexen-1-ol	Vector Control	288761233	244278702	266519968	12
	XP Plants	271501508	265268646	268385077	2
	XK Plants	149944127	138678662	144311395	6